Transcriptome and metabolome analysis provide insights into root and root released organic anion responses to phosphorus deficiency in oat

Yanliang Wang[1], Erik Lysøe[1*], Tegan Armarego-Marriott[2], Alexander Erban[2], Lisa Paruch[1], Andre van Eerde[1], Ralph Bock[2] and Jihong Liu-Clarke[1]*

1. Division of Biotechnology and Plant Health, Norwegian Institute of Bioeconomy Research, Ås, Norway
2. Max-Planck-Institute of Molecular Plant Physiology, Am Mühlenberg 1, D-14476 Potsdam-Golm, Germany

Email address of each author: Y.W., Yanliang.wang@nibio.no; T.A.M., Armarego@mpimp-golm.mpg.de ; A.E., erban@mpimp-golm.mpg.de; L.P., lisa.paruch@nibio.no; A.V.E., Andre.vanEerde@nibio.no; R.B., RBock@mpimp-golm.mpg.de

*Corresponding authors:

Research Professor Jihong Liu Clarke

Tel: +47 995 94 790 Email: Jihong.liu-clarke@nibio.no

Researcher Erik Lysøe

Tel: +47 99713274 Email: erik.lysoe@nibio.no

Total words: 5401 (Introduction: 1035 words; Materials and Methods: 1477 words; Results: 1210 words; Discussion: 1540 words; Acknowledgements: 139 words)

Total figures: 7 (Fig.4 and Fig.5 should be published in colour) Total tables: 4

Supporting information: 4 figures + 6 tables

Running title: Root transcriptome and metabolome responses to low-P in oat

Highlight

We found oat- a monocot food crop, showed high exudation rate of citrate under phosphorus deficiency; root transcriptome and metabolome were then investigated to understand oat adaptation to P deficiency.

Abstract

Root and root-released organic anions play important roles in uptake of phosphorus (P), an essential macronutrient for food production. Oat, ranking sixth in the world's cereal production, contains valuable nutritional compounds and can withstand poor soil conditions. The aim of this research was to investigate root transcriptional and metabolic responses of oat grown under P-deficient and P-sufficient conditions. We conducted a hydroponic experiment and measured root morphology, organic anions exudation, and analysed changes in the transcriptome and metabolome, to understand oat root adaptation to P deficiency. We found that oat roots showed enhanced citrate and malate exudation after four weeks of P-deficiency. After 10 days of P-deficiency, we identified 9371 differentially expressed transcripts with a two-fold or greater change ($p < 0.05$): forty-eight sequences predicted to be involved in organic anion biosynthesis and efflux were consistently up-regulated; twenty-four up-regulated transcripts in oat were also found up-regulated upon P starvation in rice and wheat under similar conditions. Phosphorylated metabolites (i.e. glucose-6-phosphate, myo-inositol-phosphate) reduced dramatically, while citrate and malate, some sugars and amino acids increased slightly in P-deficient oat roots. Our data provide new insights into the root responses to P deficiency and root-released organic anions in oat.

Keywords: metabolome, oat (*Avena sativa L.*), organic anions, phosphorus deficiency, plant roots, RNA-seq

Introduction

Oat, *Avena sativa* L., is one of the most important food and feed crops in the world. It contains various nutritional and health-promoting compounds such as avenanthramides, tocopherols (vitamin E), and digestive fibre (β-glucans) (Gutierrez-Gonzalez *et al.*, 2013; Gutierrez-Gonzalez & Garvin, 2016), which may help reduce blood pressure and blood sugar levels, reduce cholesterol, and promote healthy gut bacteria (Alminger and Eklund-Jonsson, 2008; Nazare *et al.*, 2009; Valeur *et al.*, 2016; Whitehead *et al.*, 2014). In addition, oat can withstand poor soil conditions (e.g. acidic soils; Hill 1931; Stewart and McDougall, 2014) and is widely cultivated in temperate climates.

The world population is estimated to reach 9.8 billion by 2050 (www.un.org). In order to feed the world, we need to secure sustainable food production worldwide. Phosphorus (P) is a key macronutrient with significant impact on plant growth and productivity. The application of millions of tons of P fertilizers every year exhausts the limited and non-renewable P stocks available in the world (Cordell *et al.*, 2009). Hence, an understanding of the mechanisms of P mobilization and uptake in order to improve P acquisition efficiency, particularly in staple cereal food crops, is of importance for food security, and for environmentally friendly and sustainable food production in the future (Cordell *et al.*, 2009; Faucon *et al.*, 2015; Vance *et al.*, 2003).

Plants have evolved various adaptive strategies to cope with P deficiency in nature. Examples are morphological responses such as changes in root architecture (Hermans *et al.*, 2006; Lynch, 2011); physiological adaptations like secreted organic anions and acid phosphatases (Cheng *et al.*, 2014; Gahoonia *et al.*, 2000; Hedley *et al.*, 1982; Hoffland *et al.*, 1989; Jones 1998; Lambers *et al.*, 2006; Pang *et al.*, 2015; Ryan *et al.*, 2001; Wang *et al.*, 2016), biochemical responses to optimize utilization of internal P such as replacement of P-lipids with non-P lipids (Chiou & Lin, 2011; Faucon *et al.*, 2015; Lambers *et al.*, 2015; Plaxton & Tran, 2011;), and molecular responses like induced expression of high-affinity phosphate transporters (Wu *et al.*, 2013; Zhang *et al.*, 2014). In addition, for plant species that are capable of interacting with mycorrhizal fungi, P uptake by the mycorrhizal hyphae is the dominant pathway for P acquisition (Smith *et al.*, 2003; Sawers *et al.*, 2017).

Multiple genes and different mechanisms are required to improve plant tolerance to P deficiency. Thousands of plant genes that are differentially expressed in response to P deficiency

have been identified by microarray, expressed sequence tags (EST) analysis and RNA sequencing (RNA-seq) in a large variety of plant species such as Arabidopsis (*Arabidopsis thaliana*), potato (*Solanum tuberosum*), rice (*Oryza sativa*), wheat (*Triticum aestivum*), and white lupin (*Lupinus albus*) (Hammond *et al.*, 2011; Misson *et al.*, 2005; Oono *et al.*, 2011; O'Rourke *et al.*, 2013; Oono *et al.*, 2013). Regulatory components identified include transcription factors (TFs such as PHR1), SPX domain-containing proteins, plant hormones, microRNAs, protein modifiers and epigenetic modifications (Chiou & Lin, 2011; Lin *et al.*, 2009; Panigrahy *et al.*, 2009; Wu *et al.*, 2013; Yang & Finnegan, 2010; Zhang *et al.*, 2014). The networks of regulatory genes that are necessary to sense and respond to P deficiency are complex and differ in different plant species. For Poaceae species, the molecular mechanisms associated with P uptake, translocation and remobilization are well elucidated in rice (Panigrahy *et al.*, 2009; Oono *et al.*, 2013; Wu *et al.*, 2013). Briefly, P starvation activates expression of OsPHR2, which triggers gene expression of phosphate transporters, purple acid phosphatase (PAP) and other proteins contributing to enhanced P uptake. In addition, SPX domain-containing proteins, which are activated by expression of OsPHR2, support maintenance and utilization of internal phosphate. OsPHO1 functions in P translocation (xylem loading) while SIZ1 (a small ubiquitin like modifier SUMO E3 ligase) targets PHR2 and acts both negatively and positively on various P deficiency responses. Finally, microRNA399 targets PHO2 to regulate plant P homeostasis (Chiou and Lin, 2011; Oono *et al.*, 2013; Panigrahy *et al.*, 2009; Wu *et al.*, 2013).

Plant root plays an essential role in P uptake. It is well known that to promote P uptake at reduced P availability, most species allocate more biomass to roots, increase root length and develop more and longer root hairs and later roots and so on (Hermans *et al.*, 2006; Lambers *et al.*, 2006; Lambers *et al.*, 2015; Lynch, 2011). Accordingly, mechanisms regulating root architecture like phytohormones and particularly the auxin responses under P limitation have been elucidated, as well as genes associated with those responses (see reviews Chiou and Lin, 2011; Lin *et al.*, 2009; Lynch, 2011; Panigraphy *et al.*, 2009). Root exuded organic anions is also considered as an important mechanism to mobilize soil less-available P and enhance plant P uptake, while there is little information on the molecular mechanisms involved in organic acids biosynthesis and efflux under P deficiency.

Despite the importance of oats, limited research has been carried out on its adaptation to P starvation, and particularly the molecular regulation of root and root-released organic anions in

response to P deficiency. In a previous report, we found that oat showed an increased root mass / total biomass ratio, high percentage of root colonization by arbuscular mycorrhizal fungi (AMF), large amounts of rhizosphere organic anions and efficient P uptake in low P availability soils (Wang *et al.*, 2016). These findings paved the way for our current study on the molecular mechanisms underlying P deficiency responses in oat roots and the genes and metabolites involved. Here, we compared gene expression and metabolome profiles of oat roots exposed to P sufficiency (100 μM KH_2PO_4) and deficiency (1 μM KH_2PO_4) conditions by hydroponic culture. The objectives were: 1) identification of differentially expressed transcripts in oat roots in response to P deficiency, with particular focus on up-regulated transcripts associated with organic anions biosynthesis and exudation; 2) discovery of conserved responsive genes in rice, wheat and oat, and transcripts unique for oat; 3) assessment of differential metabolite accumulation in response to P deficiency and the transcriptional program triggered by it. The overall goal of the current study was to identify candidate genes that will enrich our understanding of oat adaptation to P deficiency and that may be useful to future breeding and genetic engineering efforts towards oat improvement.

Materials and Methods

Plant growth and harvest

Seeds of the oat cultivar 'BELINDA' were germinated and grown hydroponically in full strength nutrient media (Wang *et al.*, 2015) in the greenhouse at the Norwegian University of Life Sciences. Fourteen days after sowing, seedlings were transferred to the same medium supplemented with 100 (P100) or 1 (P1) μM KH_2PO_4, respectively, and pH adjusted to 5.8±0.2. Plants were grown under a photoperiod of 16 h light and 8 h dark at a light intensity of 200 ± 20 μmol m^{-2} s^{-1} and 50-75% relative humidity, with a temperature of 25 ˚C/ 16 ˚C (day/ night). The nutrient solution was replaced every third day.

Ten days post-treatment, four root samples (representing four independent biological replications) from both P100 and P1 treated plants were collected for RNA extraction and analysis as described by Oono *et al.* (2011). The sampled roots were mixed samples containing the root cap zone, elongation zone and a part of the maturation zone. Those eight root samples, together with another eight samples (four from P1 and four from P100) were used for root metabolome analysis. When sampled roots for RNA and metabolite extraction, the roots were

quickly washed and water-removed and then immediately placed in liquid nitrogen. Additionally, eight plants (two treatments, four replicates) were used for studies of root morphology, root organic anions and biomass determinations after four weeks of different P treatments. All the plants were in vegetative growth phase, with tiller but before heading.

Root released organic anions, root morphology and biomass determination

For root exudate collection, briefly, whole root systems of intact plants were carefully washed with deionized water to remove the nutrient solution. The whole root system was then placed into ultrapure Milli-Q water (Millipore, Billerica, MA, USA) in a container to collect root exudates (Khorassani *et al*., 2011; Wang *et al*., 2015). Afterwards, micropur (0.01 g L^{-1}, Katadyn Products, Kemptthal, Switzerland) was added to the solution to inhibit the activity of microorganisms (Cheng *et al*., 2014). The collected root exudates were analysed by liquid chromatography triple quadrupole mass spectrometry (LC–MS/MS), as described in a previous study (Wang *et al*. 2015). Root released organic anions were collected and analysed after plants had been grown hydroponically under P1 or P100 for 2 weeks and 4 weeks, respectively.

After 4 weeks, the total number of green leaves and senesced leaves was recorded. For root morphology determination, WinRHIZO (EPSON 1680, WinRHIZO Pro2003b, Regent Instruments Inc., Quebec, Canada) was used to measure root length, number of lateral roots and root surface area. Shoot and root dry weight (DW) were measured separately after being oven-dried for 48 h at 65 °C. Shoot P concentrations were subsequently determined by inductively coupled plasma atomic emission spectroscopy (Wang *et al*., 2015).

RNA extraction and quality control

Total RNA was extracted using a Spectrum™ Plant Total RNA Kit (Sigma-Aldrich, St. Louis, MO, USA) and genomic DNA was removed using On-column DNase I digest kit (Sigma-Aldrich, St. Louis, MO, USA). RNA quantity and quality was assessed by a NanoDrop spectrophotometer (NanoDrop Technologies, Wilmington, DE, USA) and Agilent 2100 Bioanalyzer (Santa Clara, CA, USA). RNA samples with RIN (RNA integrity number) scores greater than 9.0 were used for RNA-Seq. Eight independent root cDNA libraries were prepared according to Illumina's TruSeq® RNA Sample Preparation v2 Guide and 125-bp paired-end reads were sequenced using an Illumina HiSeq 2500 sequencer (Illumina, San Diego, CA, USA) at the Norwegian Sequencing Centre (www.sequencing.uio.no).

171 **Sequence processing and analysis**

172 A total of 215,087,481 paired-end short read sequences were quality checked, trimmed and *de*
173 *novo* assembled using CLC Genomics Workbench v9.01 (QIAGEN Aarhus, Denmark),
174 generating 207017 contigs, with a maximum contig length of 13,319 nt, a minimum contig length
175 of 200 nt and a mean contig length of 801 nt (Table 1). Gene expression was calculated and
176 normalized using RPKM (Reads Per kb per Million reads). Differential expression between P1
177 and P100 was analyzed by *t*-tests and up-/down- regulation of genes was considered to be
178 significant if equal or greater than two-fold ($p < 0.05$). Totally, 41,679 transcripts were filtered
179 out and selected to be *de novo* Oat Root Transcriptome (*dn*ORT), used as a reference for further
180 analysis. The *dn*ORT sequences were a combination of the differentially expressed transcripts,
181 and other transcripts with RPKM $\geq$ 1.5 regardless of P treatments. These sequences were
182 annotated using Blast2Go (Conesa *et al.*, 2005) and MapMan (Thimm *et al.*, 2004). RNA
183 sequencing raw data were deposited to the GeneBank Sequence Read Archive (SRA) database
184 under bioproject identifier PRJNA355647.

185 **Real-time quantitative reverse transcription PCR (qRT-PCR) analysis**

186 First-strand cDNA was synthesized from 1.0 µg RNA using iScript™ Adv cDNA kit for qRT-
187 PCR (Bio-Rad, USA). The qRT-PCR reactions were carried out on CFX96™ Real-time system
188 (Bio-Rad, USA) using SsoAdvanced™ Universal SYBR® Green Supermix (Bio-Rad, USA) with
189 transcript-specific primers shown in Supporting Information Table S5. Ten ng cDNA were used
190 as template in a 20 µl qPCR reaction consisting of 0.8 µM primers. After initial denaturing at
191 95°C for 5 min, the reaction was followed by 40 cycles at 95°C for 15 s, 61°C for 15 s and 72°C
192 for 45 s. The expression of endogenous reference genes *EF1α* (Elongation factor 1α, Kemen *et*
193 *al.*, 2014) and *β-Actin* was used to normalize the expression level estimated by the ΔΔCq method
194 provided by CFX Manager 3.1 (Bio-Rad, USA). Four biological replicates of each treatment and
195 three technical replicates of each sample were applied in the analysis. The qPCR data were
196 represented as fold change (P1 mean value: P100 mean value) derived from relative normalized
197 expression level from four biological replicates and further compared with RNA-seq results (P1
198 RPKM means/ P100 RPKM means). *R* software (version 3.2.2) and one-way ANOVA were used
199 to examine significant differences between P1 and P100 treatments. Heat maps were generated in
200 Heml 1.0: Heatmap illustrator as described by Deng *et al.* (2014).

Root metabolite extraction

Eight replicate samples each of roots from plants grown under P1 and P100 conditions were sampled. Frozen samples (with water content varying between 95.3% and 96.6%) of 100 mg (± 10%) root were ground to homogeneity (2 min, 30 Hz; Grinding Mill MM310; Retsch, DE) under frozen conditions. To each sample was added 360 µL precooled (-20 ºC) extraction buffer (300µL methanol, 30 µL 2 mg mL^{-1} nonadecanoic acid methylester in chloroform, 30 µL 0.2 mg mL^{-1} 13-C sorbitol in methanol) and samples shaken for 15 min, 70 ºC, 1000 rpm (Thermomixer Comfort Eppendorf, DE). Samples were cooled to room temperature, added to 200 µL $CHCl_3$ and further shaken for 5 min, 37 ºC, 1000 rpm. To each sample was added 400 µL H_2O and, following vortexing, samples were centrifuged (5 min, 14000 rpm) to facilitate phase separation. Finally, 160 µL of the upper, polar phase was aliquoted and dried overnight by Speed Vac.

Gas chromatography–mass spectrometry (GC-MS) metabolite profiling and identification

Prior to gas chromatography–electron impact–time of flight mass spectrometry (GC-EI/TOF-MS) analysis, metabolites were methoxyaminated and trimethylsilylated. Briefly, addition of 40 µl MeOX (40 mg ml^{-1} methoxyaminhydrochloride in pyridine), samples were shaken (1.5 h, 30 ºC), addition of 80 µl BSTFA mixture (70 µl N, O-Bis(trimethylsilyl)trifluoroacetamide +10 µl Alkane-Mix (n-alkanes: C10, C12, C15, C18, C19, C22, C28, C32, and C36)), and further shaken (30 min, 37 ºC). GC-MS was undertaken using an Aligent CP9013 column in an Agilent 6890N24 gas chromatograph, coupled to a Pegasus III, similar to that previously described (Dethloff *et al*., 2014; Erban *et al*., 2007; Wagner *et al*., 2003). Measurements were undertaken both splitless and split (1/30) from an injection volume of 1 µL, with bulk metabolites reaching the upper detection limit in split-less measurements evaluated from split data. Retention indices were calibrated based on added n-alkanes (Strehmel *et al*., 2008).

Chromatograms were visually controlled, baseline corrected and exported in NetCDF format using ChromaTOF. Further data processing and compound identification was performed with TagFinder (Luedemann *et al*., 2008) and by matching to the Golm Metabolome Database (GMD, http://gmd.mpimpgolm.mpg.de/; Kopka *et al*., 2005; Schauer *et al*., 2005), and the NIST08 database (http://www.nist.gov/srd/mslist.htm). Manually supervised metabolite annotation and quantification was undertaken with the requirement of at least three specific quantitative mass fragments per compound, and a retention index deviation < 1.0 %. Data were normalized to

sample fresh weight, the internal 13-C6 sorbitol, and represented relative to the mean value of P100 samples per analyte.

Principal component analysis (PCA) and statistical analysis

PCA was carried out by using the program *R*. Data were normalized to the median of the P100 samples and subsequently subjected to logarithmic (Log2) transformation. Missing values were not substituted with zero or a constant value. Statistical testing was performed using the *t* test in multiple experiment viewer MeV (Saeed *et al*., 2006), based on Log2 transformed data, followed by Mann-Whitney false discovery rate (FDR) correction at $\alpha < 0.05$, due to non-normal distribution (as shown by PCA analysis) of the metabolite data.

Results

Plant growth, root morphology and root released organic anion analysis

The plant phenotype and root released organic anions were examined to study the effects of P deficiency on oat growth and root exudates under hydroponic condition. After four weeks of growth under two different P regimes (1 and 100 μM KH_2PO_4), a drastic reduction of shoots P concentration was observed in plants grown under P deficient conditions (P1), compared with P100 (0.90 vs 6.35 mg g^{-1}). Oat plants subjected to P1 treatment showed on average a 55% reduction in the total number of leaves, 44% more senescent leaves (number of senescent leaves: number of total leaves), 68% less shoot dry biomass and 96% greater root mass ratio (root dry biomass: total dry biomass) than P100 plants as shown in Fig. 1A-D. Moreover, P1 treatment plants showed shorter total root length (25%), less root surface area (27%) and more lateral roots (14%) than P100 plants (Fig. 2A-D). Furthermore, after four weeks, compared with P100 treated plants, which showed no detectable root released organic anions, P1 roots had higher exudation rates of citrate and malate, 927 and 81 nmol h^{-1} g^{-1} root dry weight (DW) respectively, as shown in Fig. 2E. By contrast, no organic anions were detected in either P1 or P100 root exudates collected after two weeks treatment.

Transcriptome analysis of root response to P deficiency

Next, RNA-seq was performed to evaluate gene expression from P deficient roots of oat plants as compared to P sufficient roots. We did Blastx and GO analyses after the *dnORT* database was constructed as described in the Material and Methods part. Approximately 9.4% of the *dn*ORT

transcripts could not be assigned to any Blastx hits (E-value > 1E-3) as shown in Supplementary Data Fig. S1. The blastx top hit species were: *Brachypodium distachyon* (22%), *Hordeum vulgare* subsp. *vulgare* (17%), *Aegilops tauschii* (15%), *Triticum urartu* (10%) and *Oryza sativa japonica* group (4%) (Fig. S2). Functional gene ontology (GO) classification of *dn*ORT sequences suggested that the biological process was mainly represented by the term 'cellular and metabolic processes', and the most represented GO subcategories within the cellular component main term were 'cell or cell part' and 'membrane or membrane part'. When the sequences were categorized according to the molecular function main term, 10,699 transcripts corresponded to 'binding category' and 10,522 sequences to 'catalytic activity' (Fig. S3). Putative functions (with InterProScan) were predicted for 62 % of the sequences (Fig. S4).

In total, 9,371 transcripts (7,817 up-regulated, 1,554 down-regulated) were differentially expressed in response to P deficiency as shown in Table 1. Gene ontology (GO) categories showed that up-regulated transcripts under P deficiency were categorized into more than 40 groups, such as oxidation-reduction process, transmembrane transport, carbohydrate metabolic process, response to osmotic stress, biosynthetic process, pyruvate metabolism, tricarboxylic acid cycle, acid phosphatase, and CCAAT-binding complex (Fig. 3).

Reciprocal tblastx (E < 1E-10) analysis showed that 24 oat transcripts which were up-regulated in P1 matched the conserved responsive genes previously found up-regulated in both rice and wheat (Oono *et al.*, 2013) as listed in Table 2. We also found 25 unique responsive transcripts (between 308 nt and 1672 nt) in oat roots that were up-regulated more than two-fold ($p < 0.001$, P1 RPKM means > 5), without any blast hits in currently available databases, i.e. they seem to be exclusively expressed in oat (Table 3).

Furthermore, as shown in Fig. 4 and Tables S1, S2, among the 7817 up-regulated transcripts, 128 transcripts were annotated as transcription factors (TFs), 57 sequences assigned as acid phosphatases and 18 as phosphate transporters. In addition, there were two sequences similar to SIZ1, SPX domain-containing proteins and PHO1 (which transfers P from roots to shoots), respectively, and one sequence was annotated as PHO2. Transcripts associated with auxin responses that regulate root development, and with disease and fungus responses, were also detected, as shown in Supporting Information Table S3.

Up-regulated transcripts associated with root-released organic anions

The citric acid and glyoxylate cycles play important roles in synthesis of organic acids in plant tissues. To see if biosynthesis of organic acids could be altered by P deficiency, we mapped the annotated transcripts to genes that involved in citric acid and glyoxylate cycles. Our analysis revealed that 38 up-regulated transcripts identified under P1 treatment represent enzyme-encoding genes putatively involved in the citric acid and glyoxylate cycles (Fig. 5A-B and Table S4). In addition, organic anions were mainly exuded through plasma membrane located transporters. Hence, we further found 10 sequences which were associated with organic anion efflux transporters including the MATE efflux family (transporters that transport a broad range of substrates such as organic anions, plant hormones and secondary metabolites), citrate transporter (CT) and ALMT (aluminium-activated malate transporter), as shown in Fig. 5C and Table S4.

RNA-seq validation by qRT-PCR

To assess whether differential expressed transcripts could be confirmed by an alternate method, 14 transcripts were selected and analysed by qRT-PCR using primers listed in Table S5. Transcripts known to be up-regulated in response to phosphate starvation, i.e. PHO2, PAP3, RNS1 (RNase), PHO1 and SPX, were confirmed by qRT-PCR which showed similar expression patterns to those analyzed by RNA-seq. Additionally, the expression of transcripts involved in root organic anion synthesis such as MSIL (malate synthase-isocitrate lyase), PEPC (phosphoenolpyruvate carboxylase), CS (citrate synthase), LMD (L-malate dehydrogenase), NADP-MD (NADP-dependent malate dehydrogenase) and efflux transporters like ALMT and MATE was also investigated by qRT-PCR. Among 14 transcripts evaluated by qRT-PCR, the trend of changes in 11 (79%) were consistent with the RNA-seq data (Fig. 6).

Metabolome Analyses

To assess the effects of gene expression in oat roots on overall metabolism, nonbiased metabolite profiling of oat roots was performed using GC-MS. We detected and identified 82 metabolites in oat roots subjected to P1 and P100, as provided in Table S6. Table 4 lists those metabolites that are significantly different ($p<0.05$, *t* test in MeV) between the P1 and P100 treatments as well as the P1/P100 response ratios (based on non-transformed data) and FDR correction (based on Log2 transformed data). The primary metabolites were amino acids, organic acids, polyhydroxy acids, sugars, phosphates, polyols, and *N*-compounds. Most of the metabolites showed a response ratio

lower than 1, indicating a decrease in P1 roots; only eight metabolites were increased in P1 roots (Table 4 and Table S6).

PCA analysis of metabolite data using all 82 known metabolites as well as 22 alternative metabolites and 39 mass spectral metabolite tags (MSTs) indicated that PC1 nicely defines the difference between two groups and represents about 35.8% of the variation (Fig.7). However, some overlap in the samples can be seen and high variation within the samples of the same group can be observed, which probably suggested different levels of P deficiency in oat roots and some P100 treated plants might be suffering P deficiency due to rapid depletion of P in the solution. After FDR correction, only five metabolites showed significant differences between P1 and P100 roots: phosphoric acid, mannose-6-phosphate, glucose-6-phosphate, glucopyranose and myo-inositol-phosphate, which indicated that the central metabolism might be stable in oat roots after 10 days of P deficiency. Regarding the organic acids, all identified organic acids showed P1/P100 ratios lower than 1 except for citric and malic acids, which showed P1/P100 ratios of 1.08 and 1.23, respectively (Table 4 and Table S6).

Discussion

Phosphorus (P) deficiency severely limits plant growth and productivity. This is especially important for sustainable staple cereal crop production in the future. Understanding the molecular mechanisms underlying root and root-secreted organic anion responses to P deficiency in oat, one of the main cereal crops in the world, is of high interest for optimizing future oat production.

Hydroponics as a root environment influences root architecture, in particular root elongation due to reduced mechanical impedance in the absence of solids (Bengough *et al*., 2001). Previous studies have suggested that root exudation by plants grown in hydroponics is different from root exudation by plants grown in soil (Neumann *et al*., 2009; Wang *et al*., 2015 & 2016). Nevertheless, the elimination of other variables such as impact of soil particles and soil microorganisms favour use of hydroponics in root exudation studies (Aulakh *et al*., 2001; Cheng *et al*., 2014; Dechassa and Schenk, 2004; Gahoonia *et al*., 2000; Ligaba *et al*., 2004). In addition, RNA-seq analysis also benefits from removing the influence of these variables on gene expression, while hydroponics use makes high quality RNA extraction easier.

Oono *et al*. (2011 & 2013) concluded that the highest number of responsive transcripts was observed in roots at 10 days after P deficiency in rice and wheat, while the plants' morphological

and physiological responses to P deficiency become prominent at around 30 days of P starvation (Cheng *et al*., 2014; Oono *et al*., 2011; Wang *et al*., 2015). Hence, we studied transcriptome and metabolome, and root morphology and exudates at different time points (i.e., 10 days for RNA and metabolome samples and two or four weeks for root exudates) after the P1 and P100 treatments. Our gene expression and metabolome profiles represent early to mid-term responses, while the others were mainly long-term P deficiency responses.

Based on our physiological analysis, we did not detect any organic anion exudation after two weeks of P-deficiency in oat. This might be due to: 1) the extracted organic anions were below the detection limit; 2) root released organic anions were affected by the plant developmental stage (Aulakh *et al*., 2001; Watt and Evans, 1999; Wang *et al*., 2017). Following four weeks of P-deficiency, under similar growth and sampling conditions, oat root had higher exudation rate of citrate than other species such as canola, rice, cabbage, carrot, barley, soybean and potato (Aulakh *et al*., 2001; Dechassa and Schenk, 2004; Gahoonia *et al*., 2000; Ligaba *et al*., 2004; Liang et al., 2013; Wang *et al.*, 2015), as well as white lupin (Cheng *et al.*, 2014; Watt and Evans, 1999; Wang *et al*., 2007) which is to our knowledge currently the most efficient species that uses root-secreted citrate to cope with P deficiency (Cheng *et al.*, 2011). Additionally, the high exudation rate of citrate by oat roots under P1 treatment corresponded well with our greenhouse experiment using clay-loam agricultural soils (Wang *et al.*, 2016). Therefore, exudation of citrate appeared to be a late response to P starvation in oat. Given that production and exudation of organic anions is a more carbon-costly process than other pathways (e.g., the production of root hairs and lateral roots) for plants (Lynch, 2007; Whipps, 1990), it might be economical to release organic anions just at a certain stage.

Transcripts encoding PEPC and malate synthase from a glyoxylate-like cycle, which are involved in organic anion production, as well as sequences assigned to citrate and malate efflux transporters were detected in the transcriptome of white lupin cluster roots under low P stress (O'Rourke *et al*., 2013). By contrast, such transcripts were not reported in wheat, rice, *Arabidopsis* or potato studies (Hammond *et al*., 2011; Oono *et al*., 2011; Oono *et al*., 2013; Misson *et al*., 2005), probably due to these plants exhibiting a low exudation rate of organic anions under P deficiency (Aulakh *et al*., 2001; Neumann and Romheld, 1999; Narang *et al*., 2000; Wang *et al*., 2015). In P starved oat roots, we identified 38 up-regulated transcripts encoding almost all enzymes associated with the citric acid and glyoxylate cycles except for

fumarase and α-ketoglutarate dehydrogenase. Moreover, a transcript annotated as malate synthase-isocitrate lyase (MSIL) was highly expressed (> 40-fold) under the P1 compared with the P100 treatment, suggesting an important role of the glyoxylate cycle in organic anion production in oat. This gene is of interest and could be used to improve P uptake in other species using genetic engineering. Exudation of organic anions may also lead to alteration of gene expression of enzymes involved in organic acid metabolism, but this is unlikely to be the case in the current study since no organic anion exudation was detected yet when we sampled RNA.

In white lupin, enhanced levels of citrate were observed in roots (2.2 fold) and cluster roots (7.6 fold) after 22 days P deficiency, whereas after 14 days P deficiency the changes were 1.4 and 3.5 fold, respectively (Müller *et al*., 2015), suggesting that changes in the metabolome mainly occurred after long-term P deficiency. Our oat root metabolome analysis indicated that most organic acids showed a general reduction after 10 days of P deficiency, which corresponded well with common bean roots after 21 days of low-P treatment (Hernández *et al*., 2007), while slight (but not significant) increases in citric and malic acids were detected in our study. Previous studies have suggested that biosynthesis and exudation of organic anions has been associated with enhanced expression of genes encoding PEPC, malate dehydrogenase, citrate synthase and transporters like ALMT and MATE (de la Fuente *et al*., 1997; Delhaize *et al*., 2009; Johnson *et al*., 1994; Koyama *et al*., 2000; Watt and Evans, 1999; Wang *et al*., 2013). However, interpretation of links between gene expression and organic acids biosynthesis and exudation should be done with caution, because enhanced gene expression does not necessarily result in enhanced enzyme levels (and enzyme activities). Also, other cellular conditions caused by P deficiency can affect endogenous enzyme function (Ryan *et al*., 2001). Additionally, although a number of studies have shown associations between organic anion efflux and internal concentrations (Hoffland *et al*., 1989; Neumann and Romheld, 1999), internal concentrations of organic anions are unlikely to directly regulate organic anions efflux in P-deficient plants (Keerthisinghe *et al*., 1998; Ryan *et al*., 2001; Watt and Evans, 1999). Rather, transporters are likely to be the most important regulators of organic anion exudation (Ryan *et al*., 2001). We identified ten up-regulated transcripts encoding MATE and ALMT family members, and other citrate and malate transporters. While higher expression of transporter-encoding genes may increase the number of transporters per cell, the expression of these transcripts was not high (0.66-16.66 RPKM), and enhanced transcript accumulation cannot be assumed to equal increased

411 protein abundance. Furthermore, efflux is determined by both abundance and activity, with
412 regulation of the latter still largely unknown.

413 Among the known genes expressed in P deficiency, a highly conserved PHR1-IPS1-
414 miRNA399-PHO2 signalling cascade has been elucidated in Arabidopsis and rice (Lin *et al.*,
415 2009; Oono *et al.*, 2013). PHR1 (PHR2 in rice) is a MYB-type transcription factor, acting as a
416 key factor in regulating downstream P deficiency responsive gene expression. Both AtPHR1 and
417 OsPHR2 were not very responsive to P deficiency, but their overexpression activated the
418 expression of a number of P-starvation induced genes even under P sufficient conditions (Rubio
419 *et al*., 2001; Zhou *et al*., 2008). We did not identify any transcript annotated as PHR1 or PHR2 in
420 our *dn*ORT database. We detected up-regulated SPX, PHO2, RNS1 and SIZ1 in oat. SPX may
421 inhibit the expression of PHR1, and SIZ1 facilitates sumoylation of PHR1 and thereby regulates
422 the post-translational modification of PHR1 (Chiou & Lin, 2011; Wu *et al.*, 2013), which likely
423 explains why we could not detect differentially expressed PHR1 in oat and suggests that the
424 PHR1-IPS1-miRNA399-PHO2 signalling cascade is likely also conserved in oat.

425 In our study, we also detected many CCAAT-box binding transcription factors, including
426 Nuclear Factor (NF) Y subunits NF-YA, NF-YB and NF-YC, which respond to P deficiency in
427 oat. CCAAT-box transcription factors, in particularly NFYA-B1, play essential roles in root
428 development and P uptake in wheat (Qu *et al.*, 2015). Our previous study also found that root
429 morphology, rhizosphere bacteria and root-colonizing mycorrhizal fungi were involved in the
430 response to low P availability in oat (Wang *et al*., 2016). The current study identified about 30
431 up-regulated transcripts associated with auxin responses, which might regulate root morphology;
432 more than 60 transcripts involved in disease response and 9 involved in responses to fungal
433 infection. Additionally, 24 up-regulated transcripts under P deficiency found in the present study
434 had been reported previously in rice and wheat (Oono *et al*. 2011 & 2013), suggesting that these
435 genes are valuable indicators of P deficiency in cereal crops. Another 25 unique transcripts in oat
436 that were up-regulated more than two-fold under P deficiency were identified. These will be
437 studied further to investigate their roles related to P uptake in oat, in order to facilitate future
438 improvements in oat production.

439 In summary, our current study provides new insights into the molecular mechanisms
440 involved in root responses to P deficiency and the release of organic anions by P-starved oat roots.

441 The novel information generated in the present study enriches our understanding of oat
442 adaptation to low P availability and contributes to future sustainable oat production.

443 **Acknowledgements**

444 This study was supported by the strategic institute program (SIS) on “Opportunities for
445 sustainable use of phosphorus in food production” at the Norwegian Institute of Bioeconomy
446 Research (NIBIO). The authors thank Marit Almvik and Monica Skogen for their kind help with
447 LC-MS/MS and RNA sample preparation, respectively. We are grateful to Prof. Nicholas Clarke
448 for linguistic correction and to the Norwegian Sequencing Centre, Oslo, Norway, for library
449 preparation and sequencing. The Norwegian Sequencing Centre, a national technology platform
450 hosted by the University of Oslo and supported by the “Functional Genomics” and “Infrastructure”
451 programs of the Research Council of Norway and the South-eastern Regional Health Authorities,
452 provided the sequencing service. We thank Ines Fehrle and Joachim Kopka (both from Max
453 Planck Institute of Molecular Plant Physiology, DE) for their excellent technical assistance and
454 support in analysis of oat metabolites.

455 **Author Contributions**

456 Y.W. contributed to the experimental design, sample preparation, plant biomass and root
457 morphology measurements, data analyses and manuscript writing; J.L.C. contributed to the
458 experimental design and conceived the study; E.L. did the sequence trimming, *de novo* assembly,
459 annotation, and helped with the data analyses; T.A-M and A.E conducted metabolite
460 measurements; L.P. helped with the qRT-PCR experiment. All authors revised and approved the
461 final manuscript.

References

Alminger M, Eklund-Jonsson C. 2008. Whole-grain cereal products based on a high-fibre barley or oat genotype lower post-prandial glucose and insulin responses in healthy humans. European Journal of Nutrition **47**(6), 294-300.

Aulakh MS, Wassmann R, Bueno C, Kreuzwieser J, Rennenberg H. 2001. Characterization of Root Exudates at Different Growth Stages of Ten Rice Cultivars. Plant Biology **3**,139-148.

Bengough AG, McKenzie BM, Hallett PD, Valentine TA. 2011. Root elongation, water stress, and mechanical impedance: a review of limiting stresses and beneficial root tip traits. Journal of Experimental Botany **62**, 59-68.

Cheng L, Bucciarelli B, Shen J, Allan D, Vance CP. 2011. Focus Issue on Phosphorus Plant Physiology: Update on Lupin Cluster Roots. Update on White Lupin Cluster Root Acclimation to Phosphorus Deficiency. Plant Physiology **156**(3), 1025.

Cheng L, Tang X, Vance CP, White PJ, Zhang F, Shen J. 2014. Interactions between light intensity and phosphorus nutrition affect the phosphate-mining capacity of white lupin (*Lupinus albus* L.). Journal of Experimental Botany **65**(12), 2995-3003.

Chiou T-J, Lin S-I. 2011. Signaling network in sensing phosphate availability in plants. Annual Review of Plant Biology **62**, 185-206.

Conesa A, Götz S, García-Gómez JM, Terol J, Talón M, Robles M. 2005. Blast2GO: a universal tool for annotation, visualization and analysis in functional genomics research. Bioinformatics **21**(18), 3674-3676.

Cordell D, Drangert J-O, White S. 2009. The story of phosphorus: global food security and food for thought. Global Environmental Change **19**(2), 292-305.

Dechassa N, Schenk MK. 2004. Exudation of organic anions by roots of cabbage, carrot, and potato as influenced by environmental factors and plant age. Journal of Plant Nutrition and Soil Science **167**, 623-629.

Delhaize E, Taylor P, Hocking PJ, Simpson RJ, Ryan PR, Richardson AE. 2009. Transgenic barley (Hordeum vulgare L.) expressing the wheat aluminium resistance gene (TaALMT1) shows enhanced phosphorus nutrition and grain production when grown on an acid soil. Plant Biotechnology Journal **7**(5), 391-400.

Deng W, Wang Y, Liu Z, Cheng H, Xue Y. 2014. HemI: a toolkit for illustrating heatmaps. PLos One **9**(11), e111988.

de la Fuente JM, Ramirez-Rodriguze V, Cabrera-Ponce JL, Herrera-Estrella L. 1997. Aluminum tolerance in transgenic plants by altering of citrate synthesis. Science **276**,1566-1568.

Erban A, Schauer N, Fernie AR, Kopka J. 2007. Nonsupervised construction and application of mass spectral and retention time index libraries from time-of-flight gas chromatographymass spectrometry metabolite profiles. Methods in Molecular Biology **358**, 19-38.

Faucon M-P, Houben D, Reynoird J-P, Mercadal-Dulaurent A-M, Armand R, Lambers H. 2015. Advances and Perspectives to Improve the Phosphorus Availability in Cropping Systems for Agroecological Phosphorus Management. Advances in Agronomy: Academic Press.

Gahoonia TS, Asmar F, Giese H, Gissel-Nielsen G, Nielsen NE. 2000. Root-released organic acids and phosphorus uptake of two barley cultivars in laboratory and field experiments. European Journal of Agronomy **12**(3), 281-289.

Gutierrez-Gonzalez JJ, Garvin DF. 2016. Subgenome-specific assembly of vitamin E biosynthesis genes and expression patterns during seed development provide insight into the evolution of oat genome. Plant Biotechnology Journal **14**(11), 2147-2157.

Gutierrez-Gonzalez JJ, Tu ZJ, Garvin DF. 2013. Analysis and annotation of the hexaploid oat seed transcriptome. BMC Genomics **14**, 471.

Hammond JP, Broadley MR, Bowen HC, Spracklen WP, Hayden RM, White PJ. 2011. Gene expression changes in phosphorus deficient potato (*Solanum tuberosum* L.) leaves and the potential for diagnostic gene expression markers. PLoS One **6**(9), e24606.

Hedley M, White R, Nye P. 1982. Plant-induced changes in the rhizosphere of rape (*Brassica napus* var. Emerald) seedlings. New Phytologist **91**(1), 45-56.

Hermans C, Hammond JP, White PJ, Verbruggen N. 2006. How do plants respond to nutrient shortage by biomass allocation? Trends in Plant Science **11**(12), 610-617.

Hernández G, Ramírez M, Valdés-López O, et al. 2007. Phosphorus stress in common bean: root transcript and metabolic responses. Plant Physiology **144**, 752-767.

Hill DD. 1931. Oat production in Western Oregon. ir.library.oregonstate.edu

Hoffland E, Findenegg GR, Nelemans JA. 1989. Solubilization of rock phosphate by rape. Plant and Soil **113**(2), 155-160.

Johnson JF, Allan DL, Vance CP. 1994. Phosphorus stress-induced proteoid roots show altered metabolism in *lupinus albus*. Plant Physiology **104**, 657-665.

Jones DL. 1998. Organic acids in the rhizosphere–a critical review. Plant and Soil **205**(1), 25-44.

Keerthisinghe G, Hocking PJ, Ryan PR, Delhaize E. 1998. Effect of phosphorus supply on the formation and function of proteoid roots of white lupin. Plant Cell and Environment **21**, 467-478.

Kemen AC, Honkanen S, Melton RE, Findlay KC, Mugford ST, Hayashi K, Haralampidis K, Rosser SJ, Osbourn A. 2014. Investigation of triterpene synthesis and regulation in oats reveals a

role for β-amyrin in determining root epidermal cell patterning. Proceedings of the National Academy of Sciences **111**(23), 8679-8684.

Kopka J, Schauer N, Krueger S, et al. 2005. GMD@CSB.DB: the Golm Metabolome Database. Bioinformatics **21**, 1635-1638.

Koyama H, Kawamura A, Kihara T, Hara T, Takita E. 2000. Overexpression of mitochondrial citrate synthase in Arabidopsis thaliana improved growth on a phosphorus limited soil. Plant Cell and Physiology **40**, 482-488.

Lambers H, Clode P, Hawkins H, Laliberté E, Oliveira R, Reddell P, Shane M, Stitt M, Weston P. 2015. Metabolic adaptations of the non-mycotrophic Proteaceae to soil with a low phosphorus availability: Phosphorus Metabolism in Plants in the Post-genomic Era: From Gene to Ecosystem. Wiley-Blackwell, Oxford, UK.

Lambers H, Shane MW, Cramer MD, Pearse SJ, Veneklaas EJ. 2006. Root structure and functioning for efficient acquisition of phosphorus: Matching morphological and physiological traits. Annals of Botany **98**(4), 693-713.

Liang C, Piñeros MA, Tian J, Yao Z, Sun L, Liu J, Liao H. 2013. Low pH, aluminum, and phosphorus coordinately regulate malate exudation through GmALMT1 to improve soybean adaptation to acid soils. Plant Physiology **161**,1347-1361.

Ligaba A, Shen H, Shibata K, Yamamoto Y, Tanakamaru S, Matsumoto H. 2004. The role of phosphorus in aluminium-induced citrate and malate exudation from rape (Brassica napus). Physiologia Plantarum **120**, 575-584.

Lin WY, Lin SI, Chiou TJ. 2009. Molecular regulators of phosphate homeostasis in plants. Journal of Experimental Botany **60**(5),1427-1438.

López-Bucio J, Nieto-Jacobo MaF, Ramírez-Rodríguez V, Herrera-Estrella L. 2000. Organic acid metabolism in plants: from adaptive physiology to transgenic varieties for cultivation in extreme soils. Plant Science **160**(1), 1-13.

Luedemann A, Strassburg K, Erban A, Kopka J. 2008. TagFinder for the quantitative analysis of gas chromatography-mass spectrometry (GC-MS)-based metabolite profiling experiments. Bioinformatics **24**, 732-737.

Lynch JP. 2007. Roots of the second green revolution. Australian Journal of Botany **55**, 493-512.

Lynch JP. 2011. Root phenes for enhanced soil exploration and phosphorus acquisition: tools for future crops. Plant Physiology **156**(3), 1041-1049.

Misson J, Raghothama KG, Jain A, Jouhet J, Block MA, Bligny R, Ortet P, Creff A, Somerville S, Rolland N. 2005. A genome-wide transcriptional analysis using *Arabidopsis thaliana* Affymetrix

gene chips determined plant responses to phosphate deprivation. Proceedings of the National Academy of Sciences USA **102**(33), 11934-11939.

Miura K, Rus A, Sharkhuu A, Yokoi S, Karthikeyan AS, Raghothama KG, Yun DJ. 2005. The Arabidopsis SUMO E3 ligase SIZ1 controls phosphate deficiency responses. Proceedings of the National Academy of Sciences USA **102**(21), 7760-7765.

Müller J, Gödde V, Niehaus K and Zörb C. 2015. Metabolic Adaptations of White Lupin Roots and Shoots under Phosphorus Deficiency. Frontiers in Plant Science. **6**, 1014. doi: 10.3389/fpls.2015.01014

Narang RA, Bruene A, Altmann T. 2000. Analysis of phosphate acquisition efficiency in different Arabidopsis accessions. Plant Physiology **124**(4), 1786-1799.

Nazare JA, Normand S, Oste Triantafyllou A, Brac de la Perrière A, Desage M, Laville M. 2009. Modulation of the postprandial phase by beta-glucan in overweight subjects: effects on glucose and insulin kinetics. Molecular Nutrition & Food Research **53**(3), 361-369.

Nazeri NK, Lambers H, Tibbett M, Ryan MH. 2014. Moderating mycorrhizas: arbuscular mycorrhizas modify rhizosphere chemistry and maintain plant phosphorus status within narrow boundaries. Plant Cell and Environment **37**(4), 911-921.

Neumann G, Romheld V. 1999. Root excretion of carboxylic acids and protons in phosphorus deficient plants. Plant and Soil **211**, 121-130.

Neumann G, George T, Plassard C. 2009. Strategies and methods for studying the rhizosphere—the plant science toolbox. Plant and Soil **321**, 431–456.

O'Rourke JA, Yang SS, Miller SS, et al. 2013. An RNA-Seq transcriptome analysis of orthophosphate-deficient white lupin reveals novel insights into phosphorus acclimation in plants. Plant Physiology **161**(2), 705-724.

Oono Y, Kawahara Y, Kanamori H, Mizuno H, Yamagata H, Yamamoto M, Hosokawa S, Ikawa H, Akahane I, Zhu Z. 2011. mRNA-Seq reveals a comprehensive transcriptome profile of rice under phosphate stress. Rice **4**(2), 50-65.

Oono Y, Kobayashi F, Kawahara Y, Yazawa T, Handa H, Itoh T, Matsumoto T. 2013. Characterisation of the wheat (*Triticum aestivum* L.) transcriptome by de novo assembly for the discovery of phosphate starvation-responsive genes: gene expression in Pi-stressed wheat. BMC Genomics **14**(1), 1-14.

Pandey R, Meena SK, Krishnapriya V, Ahmad A, Kishora N. 2014. Root carboxylate exudation capacity under phosphorus stress does not improve grain yield in green gram. Plant Cell Reports **33**(6), 919-928.

Pang J, Yang J, Lambers H, Tibbett M, Siddique KH, Ryan MH. 2015. Physiological and morphological adaptations of herbaceous perennial legumes allow differential access to sources of varyingly soluble phosphate. Physiologia Plantarum **154**(4), 511-525.

Panigrahy M, Rao DN, Sarla N. 2009. Molecular mechanisms in response to phosphate starvation in rice. Biotechnology Advances **27**(4), 389-397.

Pearse SJ, Veneklaas EJ, Cawthray G, Bolland MD, Lambers H. 2007. Carboxylate composition of root exudates does not relate consistently to a crop species' ability to use phosphorus from aluminium, iron or calcium phosphate sources. New Phytologist **173**(1), 181-190.

Plaxton WC, and Tran HT. 2011. Metabolic adaptations of phosphate-starved plants. Plant Physiology **156**(3), 1006-1015.

Qu B, He X, Wang J, Zhao Y, Teng W, Shao A, Zhao X, Ma W, Wang J, Li B. 2015. A wheat CCAAT box-binding transcription factor increases the grain yield of wheat with less fertilizer input. Plant Physiology **167**(2), 411-423.

Rubio V, Linhares F, Solano R, Martín AC, Iglesias J, Leyva A, Paz-Ares J. 2001. A conserved MYB transcription factor involved in phosphate starvation signaling both in vascular plants and in unicellular algae. Genes & Development **15**(16), 2122-2133.

Ryan P, Delhaize E, Jones D. 2001. Function and mechanism of organic anion exudation from plant roots. Annual Review of Plant Biology **52**(1), 527-560.

Saeed AI, Bhagabati NK, Braisted JC, et al. 2006. TM4 microarray software suite. Methods in Enzymology **411,** 134-193.

Sawers RJ, Svane SF, Quan C, et al. 2017. Phosphorus acquisition efficiency in arbuscular mycorrhizal maize is correlated with the abundance of root-external hyphae and the accumulation of transcripts encoding PHT1 phosphate transporters. New Phytologist **214**(2), 632-643.

Schauer N, Steinhauser D, Strelkov S, et al. 2005. GC-MS libraries for the rapid identification of metabolites in complex biological samples. FEBS Letter **579**, 1332-1337.

Smith SE, Smith FA, Jakobsen I. 2003. Mycorrhizal fungi can dominate phosphate supply to plants irrespective of growth responses. Plant Physiology **133**(1), 16-20.

Stewart D and McDougall G. 2014. Oat agriculture, cultivation and breeding targets: implications for human nutrition and health. British Journal of Nutrition **112**, S50-57.

Strehmel N, Hummel J, Erban A, Strassburg K, Kopka J. 2008. Retention index thresholds for compound matching in GC-MS metabolite profiling. Journal of Chromatography. B, Analytical Technologies in the Biomedical and Life Sciences **871**, 182-190.

Thimm O, Bläsing O, Gibon Y, Nagel A, Meyer S, Krüger P, Selbig J, Müller LA, Rhee SY, Stitt M. 2004. MAPMAN: a user-driven tool to display genomics data sets onto diagrams of metabolic pathways and other biological processes. Plant Journal **37**(6), 914-939.

Valeur J, Puaschitz NG, Midtvedt T, Berstad A. 2016. Oatmeal porridge: impact on microflora-associated characteristics in healthy subjects. British Journal of Nutrition **115**(1), 62-67.

Vance CP, Uhde-Stone C, Allan DL. 2003. Phosphorus acquisition and use: critical adaptations by plants for securing a nonrenewable resource. New Phytologist **157**(3), 423-447.

Wagner C, Sefkow M, Kopka J. 2003. Construction and application of a mass spectral and retention time index database generated from plant GC/EI-TOF-MS metabolite profiles. Phytochemistry **62**, 887-900.

Wang BL, Shen JB, Zhang WH, Zhang FS, Neumann G. 2007. Citrate exudation from white lupin induced by phosphorus deficiency differs from that induced by aluminum. New Phytologist **176**, 581-589.

Wang Y, Krogstad T, Clarke N, **Øgaard A, Clarke JL**. 2017. Impact of phosphorus on rhizosphere organic anions of wheat at different growth stages under field conditions. AoB Plants **9** (plx008). Doi: 10.1093/aobpla/plx008

Wang Y, Krogstad T, Liu Clarke J, Hallama M, Øgaard A, Eich-Greatorex S, Kandeler E, Clarke N. 2016. Rhizosphere organic anions play a minor role in improving crop species' ability to take up residual phosphorus (P) in agricultural soils low in P availability. Fronters in Plant Science **7**(1664). doi: 10.3389/fpls.2016.01664

Wang Y, Xu H, Kou J, Shi L, Zhang C, Xu F. 2013. Dual effects of transgenic Brassica napus overexpressing CS gene on tolerances to aluminum toxicity and phosphorus deficiency. Plant and Soil **362**(1-2), 231-246.

Wang YL, Almvik M, Clarke N, Eich-Greatorex S, Ogaard AF, Krogstad T, Lambers H, Clarke JL. 2015. Contrasting responses of root morphology and root-exuded organic acids to low phosphorus availability in three important food crops with divergent root traits. AoB Plants **7** (plv097). doi: 10.1093/aobpla/plv097

Watt M, Evans JR. 1999. Linking Development and Determinacy with Organic Acid Efflux from Proteoid Roots of White Lupin Grown with Low Phosphorus and Ambient or Elevated Atmospheric CO2 Concentration. Plant Physiology **120**, 705-716.

Whipps JM. 1990. Carbon economy. Book chapter of The rhizosphere. 59-97.

Whitehead A, Beck EJ, Tosh S, Wolever TM. 2014. Cholesterol-lowering effects of oat β-glucan: a meta-analysis of randomized controlled trials. The American Journal of Clinical Nutrition **100**(6),1413-1421.

Wu P, Shou H, Xu G, Lian X. 2013. Improvement of phosphorus efficiency in rice on the basis of understanding phosphate signaling and homeostasis. Current Opinion in Plant Biology **16**(2), 205-212.

Yang XJ, Finnegan PM. 2010. Regulation of phosphate starvation responses in higher plants. Annals of Botany **105**(4), 513-526.

Zhang Z, Liao H, Lucas WJ. 2014. Molecular mechanisms underlying phosphate sensing, signaling, and adaptation in plants. Journal of Integrative Plant Biology **56**(3), 192-220.

Zhou J, Jiao F, Wu Z, Li Y, Wang X, He X, Wu P. 2008. OsPHR2 is involved in phosphate-starvation signaling and excessive phosphate accumulation in shoots of plants. Plant Physiology **146**(4), 1673-1686.

Supplementary Data

The following supplementary data is available for this article:

Fig. S1 Data distribution of Blastx hits of *dn*ORT sequences.

Fig. S2 The Blastx top-hit species distribution of *dn*ORT sequences.

Fig. S3 Functional gene onthology (GO) classification of *dn*ORT sequences.

Fig. S4 Putative functions (with InterProScan) distribution of *dn*ORT sequences.

Table S1. Up-regulated transcription factors under P deficiency.

Table S2. Up-regulated transcripts predicted to be acid phosphatases (APases), phosphate transporters and other known genes related to P deficiency.

Table S3. Up-regulated transcripts associated with auxin responses, disease responses and responses to fungal infection under P deficiency.

Table S4. Up-regulated transcripts associated with organic anion production and efflux under P deficiency.

Table S5. Primers used in the present study.

Table S6. GC-MS metabolite profiles.

Figure Legends

Figure 1. Plant growth response to P1 and P100 treatments. (**A**) Total leaves, (**B**) Senescent leaves, (**C**) Shoot dry weight, and (**D**) Root mass ratio. Error bars indicate SE (n = 4). Significant differences are indicated (ns, not significant; ***, $p < 0.001$).

Figure 2. Oat root response to P1 and P100 treatments. (**A**) Representative photos of root structure, (**B**) Root length, (**C**) Root surface area, (**D**) Number of root tips, and (**E**) Root released organic anions. Error bars indicate SE (n = 4). Significant differences are indicated (ns, not significant; ***, $p < 0.001$).

Figure 3. Functional annotation of up-regulated sequences based on gene ontology (GO) categorization. *y*-axis indicates the category, *x*-axis the percentage of transcripts in a category.

Figure 4. Heat map of expression profiling of up-regulated transcription factors (TFs) and selected known genes related to P deficiency. P1 induced up-regulated ($p < 0.05$) TFs (**A**) and sequences assigned to APases, phosphate transporters (PHT), SPX protein, SIZ1 and PHO1 (**B**). Note that transcripts with RPKM < 3 are presented in Supporting Information Tables S1 and S2. The colour bar indicates the expression levels [represented as log2 (RPKM means)], red colour indicates high expression level while blue indicates low expression level.

Figure 5. Up-regulated sequences associated with organic anion production and efflux under P deficiency (P1). (**A**) Schematic representation of metabolic pathways including citric acid and glyoxylate cycles related to organic anion production that were up-regulated ($p < 0.05$) under P1 (**B**) and up-regulated organic anion transporters responsive to P deficiency (**C**). The colour bar indicates the expression levels [represented as log2 (RPKM means)], red colour indicates high expression level while blue indicates low expression level and black colour indicates RPKM=0.

Figure 6. Expression of candidate known genes related to low P stress, and up-regulated transcripts associated with organic anion production and efflux under P1 as determined using RNA-Seq and qRT-PCR. Fourteen genes were selected and analysed using qRT-PCR for both P1 and P100 treatments. Transcript expression levels were normalized using the internal controls β-actin and EF1α (see Methods section). Relative expression values were calculated based on means of four biological replicates (with three technical replicates) under P1 and P100

treatments. Transcripts with statistically insignificant (p >0.05) changes in expression compared with P100 roots are denoted as ns. Fold changes based on RPKM values derived from RNA-seq are plotted on the same graph. The transcript IDs for each gene are listed in Supporting Information Table S5.

Figure 7. Principal component (PC) scores of metabolic variances in oat roots (n=8 × 2). Oat plants grown in P1(circles) and P100 (triangles) solutions for 10 days were used.

Table 1. Transcriptome statistics.

Total number of reads	215,087,481
Assembled contigs	207,017
Minimum length (nt)	200
Maximum length (nt)	13,319
Mean length (nt)	801
Contigs larger than 1,000 nt	9631
Up-regulated contigs	7,817
Down-regulated contigs	1,554
Annotated contigs	41,679

nt: nucleotides

Table 2. Conserved responsive transcripts found in oat, wheat and rice under P deficiency.

*dn*ORT ID	Rice proteins	Wheat_proteins (TRIAE_CS42)	P1 RPKM	P100 RPKM	Fold change P1/P100	Gene	Gene annotation
Contig000022	Os05t0137400-01	1AS_TGACv1_020885_AA0080310.2.1	107.9	48.1	2.2		Similar to aspartic protease precursor
Contig000835	Os05t0387200-01	1DL_TGACv1_061485_AA0196630.2.1	13.5	1.7	8.0	SQD1	Sulphite: UDP-glucose sulfotr-ansferase
Contig010807	Os10t0500600-01	1DL_TGACv1_062297_AA0212030.5.1	48.3	22.6	2.1		Zinc finger, C2H2-like domain containing protein
Contig011660	Os07t0100300-02	2AL_TGACv1_094153_AA0293430.1.1	17.4	1.3	13.4		Glycosyl transferase, group 1 domain containing protein
Contig009578	Os10t0100500-01	2AS_TGACv1_113238_AA0353330.1.1	61.3	11.4	5.4		Serine/threonine protein kinase-related domain containing protein
Contig001778	Os07t0622200-01	2AS_TGACv1_113290_AA0354140.2.1	71.8	68.0	1.1		Similar to M-160-u1_1
Contig009737	Os07t0630400-01	2BS_TGACv1_146583_AA0468610.1.1	5.2	1.1	4.8	OsRNS1	Ribonuclease T2 family protein
Contig005229	Os04t0555300-01	2DL_TGACv1_158105_AA0509380.4.1	41.6	9.1	4.6		Similar to glycerol 3-phosphate permease
Contig019750	Os04t0652700-01	2DL_TGACv1_158583_AA0522480.2.1	4.8	1.2	4.0		Similar to nuclease PA3
Contig061747	Os01t0128200-01	3AS_TGACv1_210696_AA0677330.2.1	4.0	1.4	2.8		Similar to nuclease I
Contig013859	Os01t0897200-04	3B_TGACv1_224141_AA0792910.2.1	68.9	21.8	3.2	OsRNS2	Ribonuclease 2 precursor
Contig004306	Os06t0115600-01	4AL_TGACv1_289135_AA0965550.1.1	76.7	53.6	1.4		Similar to CYCLOPS
Contig026884	Os08t0299400-01	4AL_TGACv1_289998_AA0980080.1.1	13.9	0.0		MGD	MGDG synthase type A
Contig003298	Os03t0238600-01	4AS_TGACv1_308481_AA1028160.1.1	273.2	54.6	5.0	PAP	Similar to purple APase
Contig007532	Os09t0553200-01	5AL_TGACv1_374888_AA1211020.2.1	504.8	181.3	2.8	UGPase	UDP-glucose pyrophosphorylase
Contig003667	Os09t0478300-01	5AL_TGACv1_376126_AA1232370.2.1	17.7	7.5	2.4		Conserved hypothetical protein
Contig026720	Os12t0554500-00	5AS_TGACv1_393365_AA1271860.2.1	11.6	0.1	167.7		Lipase, class 3 family protein
Contig116061	Os09t0379900-02	5BL_TGACv1_404442_AA1299920.1.1	1.6	0.6	2.5		Endo-1,3(4)-beta-glucanase 2 like
Contig073770	Os08t0433200-01	5BL_TGACv1_404654_AA1307490.1.1	28.0	5.4	5.1		Conserved hypothetical protein
Contig007245	Os09t0315700-01	5BL_TGACv1_407230_AA1354660.1.1	58.1	20.4	2.9		Phosphoenolpyruvate carboxylase family protein
Contig000670	Os02t0809800-01	6BL_TGACv1_501820_AA1620890.2.1	70.5	22.9	3.1	PHO1:H2	Root-to-shoot inorganic phosphate (Pi) transfer
Contig000259	Os06t0178900-01	7BS_TGACv1_592527_AA1939830.5.1	184.6	82.2	2.2		Vacuolar H^+ −pyrophosphatase
Contig027611	Os05t0489900-01	U_TGACv1_641100_AA2085080.2.1	13.9	6.4	2.2		Calcium/calmodulin-dependent protein kinase
Contig044047	Os09t0321200-00	U_TGACv1_642666_AA2121200.1.1	0.9	0.1	11.0		Similar to carotenoid cleavage dioxygenase

Table 3. Unique P responsive transcripts found in oat.

Oat transcript ID	*p*-value	P1 - RPKM	P100 - RPKM	Fold change P1/P100	Transcript length (nt)
Contig000170	0.0001	339.8	7.6	44.5	486
Contig001596	0.0005	27.8	12.0	2.3	582
Contig002497	0.0001	10.3	1.4	7.5	452
Contig005093	0.0007	193.8	42.9	4.5	567
Contig006100	0.0001	80.8	2.0	39.6	308
Contig006686	0.0000	60.8	1.0	59.6	400
Contig007919	0.0002	67.4	0.5	134.2	586
Contig009266	0.0003	5.2	0.1	35.3	1017
Contig010063	0.0001	32.0	13.9	2.3	1256
Contig011518	0.0000	16.3	0.6	28.0	978
Contig022489	0.0000	13.6	0.0	907.5	1198
Contig023173	0.0005	116.7	47.5	2.5	410
Contig024878	0.0002	52.3	23.6	2.2	454
Contig024909	0.0005	7.3	0.1	81.8	1004
Contig029950	0.0001	8.9	0.4	24.7	817
Contig034195	0.0003	17.7	8.4	2.1	812
Contig035653	0.0004	5.5	1.7	3.1	702
Contig039702	0.0005	8.3	0.7	11.6	447
Contig040117	0.0000	14.3	0.2	77.4	630
Contig040132	0.0000	7.2	0.0	--	402
Contig045423	0.0000	7.0	0.0	--	410
Contig045562	0.0005	5.7	1.5	3.7	1672
Contig052573	0.0001	5.4	2.2	2.4	673
Contig068492	0.0001	23.4	3.2	7.3	474
Contig068533	0.0001	6.4	2.4	2.7	1167

Table 4. Known metabolites identified by GC-MS in oat roots from P1 and P100 treated plants with $p < 0.05$.

Class	Metabolite	Response ratio P1/P100	*p* value
Organic acids	2-hydroxy-glutaric acid	0.10	0.0023
	2-oxo-glutaric acid	0.08	0.0117
	Pantothenic acid	0.69	0.0118
	Pyruvic acid	0.17	0.0101
	Succinic acid	0.32	0.0063
Amino acids	4-amino-butanoic acid	0.81	0.0209
	Methionine	0.25	0.0253
	Valine	0.35	0.0460
***N*-compounds**	5-methylthio-adenosine	0.22	0.0087
	Putrescine	0.29	0.0063
	Spermidine	0.56	0.0446
Phenylpropanoids	4-hydroxy-cinnamic acid	0.75	0.0372
Phosphates	Ethanolaminephosphate	0.30	0.0404
	Fructose-6-phosphate	0.43	0.0063
	Glucose-6-phosphate	0.19	**0.0011**
	Glycerophosphoglycerol	0.27	0.0367
	Mannose-6-phosphate	0.22	**0.0011**
	myo-Inositol-phosphate	0.25	**0.0016**
	Phosphoric acid	0.28	**7.8E-4**
	Phosphoric acid monomethyl ester	0.41	0.0118
	Glucose-6-phosphate	0.20	0.0034
Polyhydroxy Acids	Lyxonic acid	0.48	0.0039
	Ribonic acid	0.45	0.0087
Polyols	Arabitol	0.56	0.0087
	Inositol, myo-	0.84	0.0157
	Ribitol	0.49	0.0157
Sugars	Sucrose	0.47	0.0357
	Xylose	0.65	0.0209
	Glucopyranose	0.27	**0.0016**
	Maltose	0.53	0.0207

FDR correction with $\alpha < 0.05$ is indicated by bold format of the *p* value.

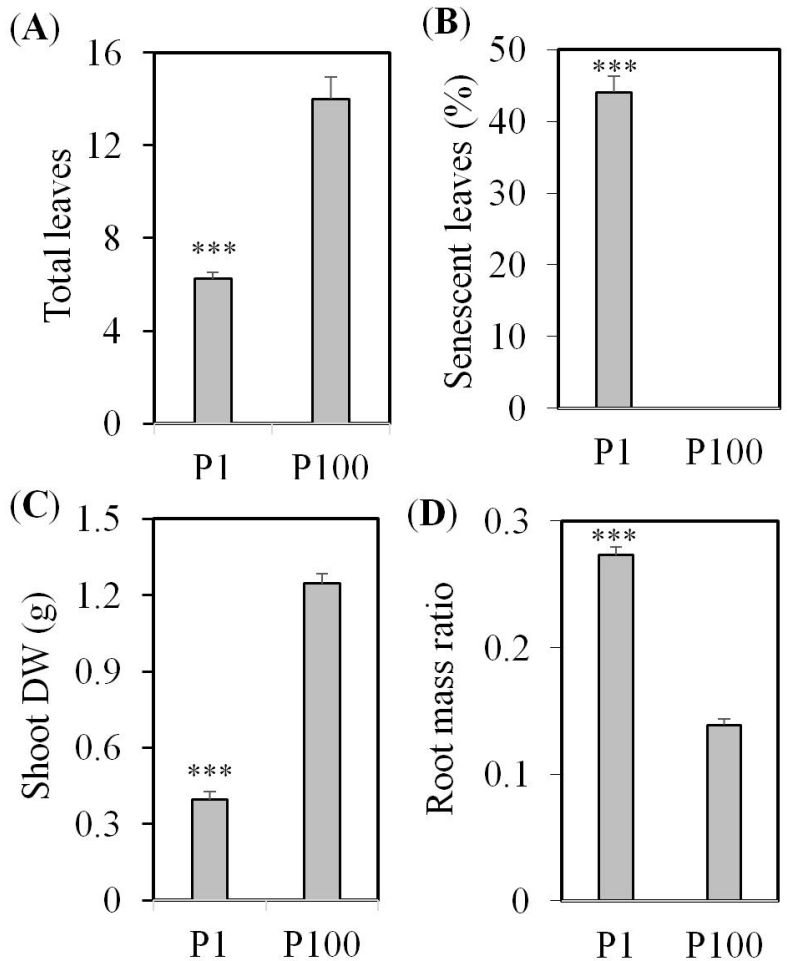

Wang *et al.*, Fig.1

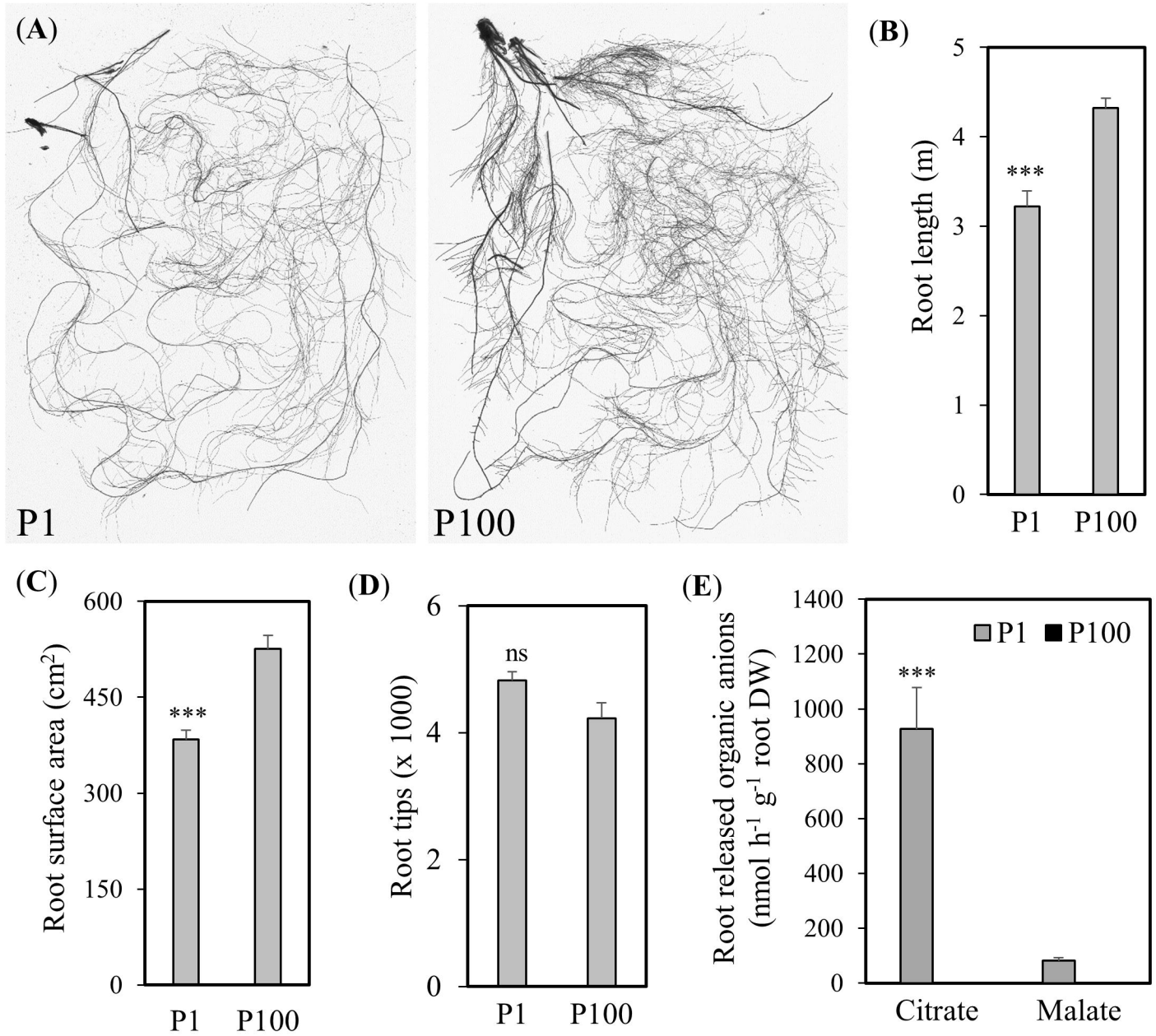

Wang *et al.*, Fig.2

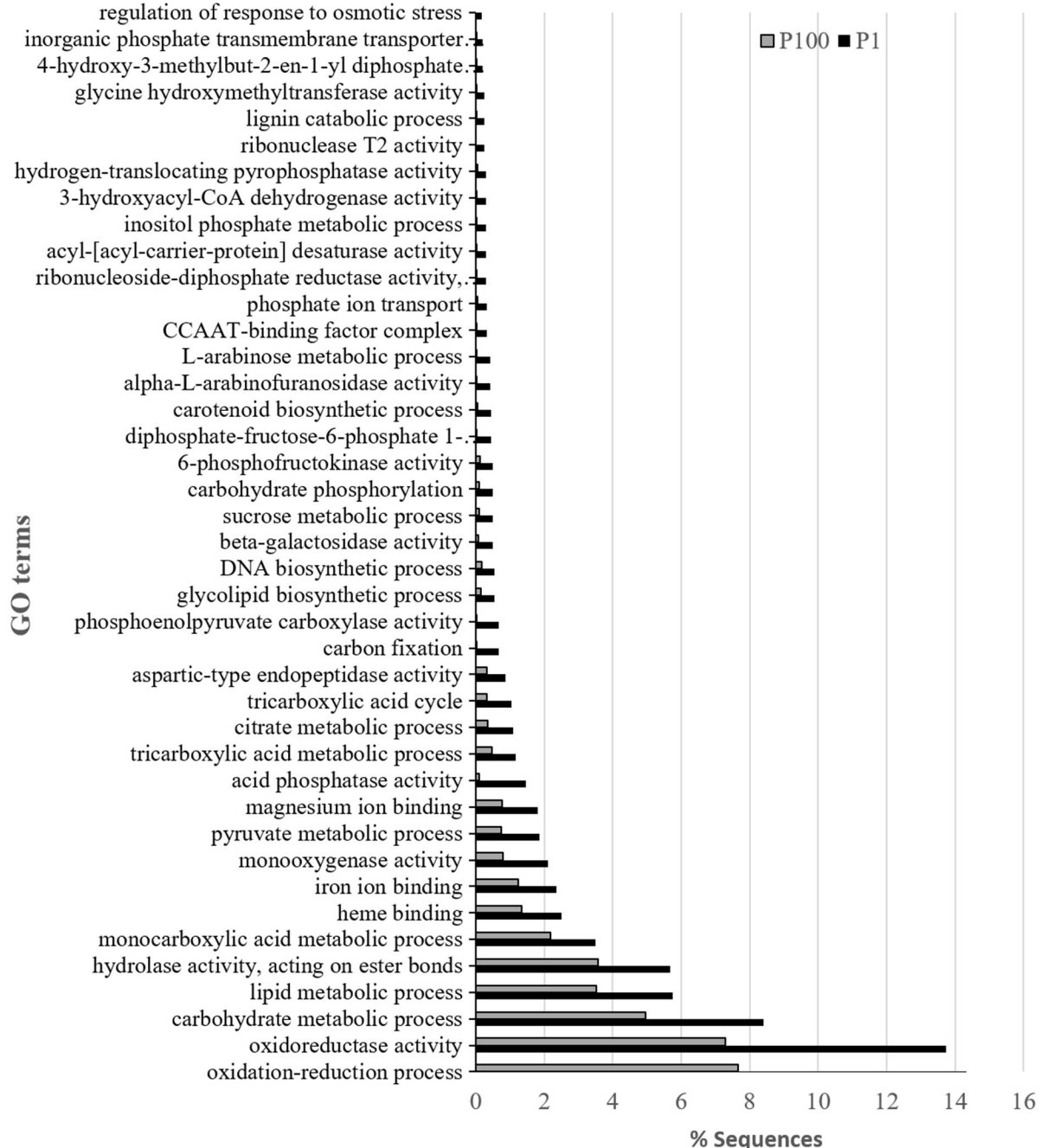

Wang *et al.*, Fig.3

Wang *et al.*, Fig.4A

Wang *et al.*, Fig.4B

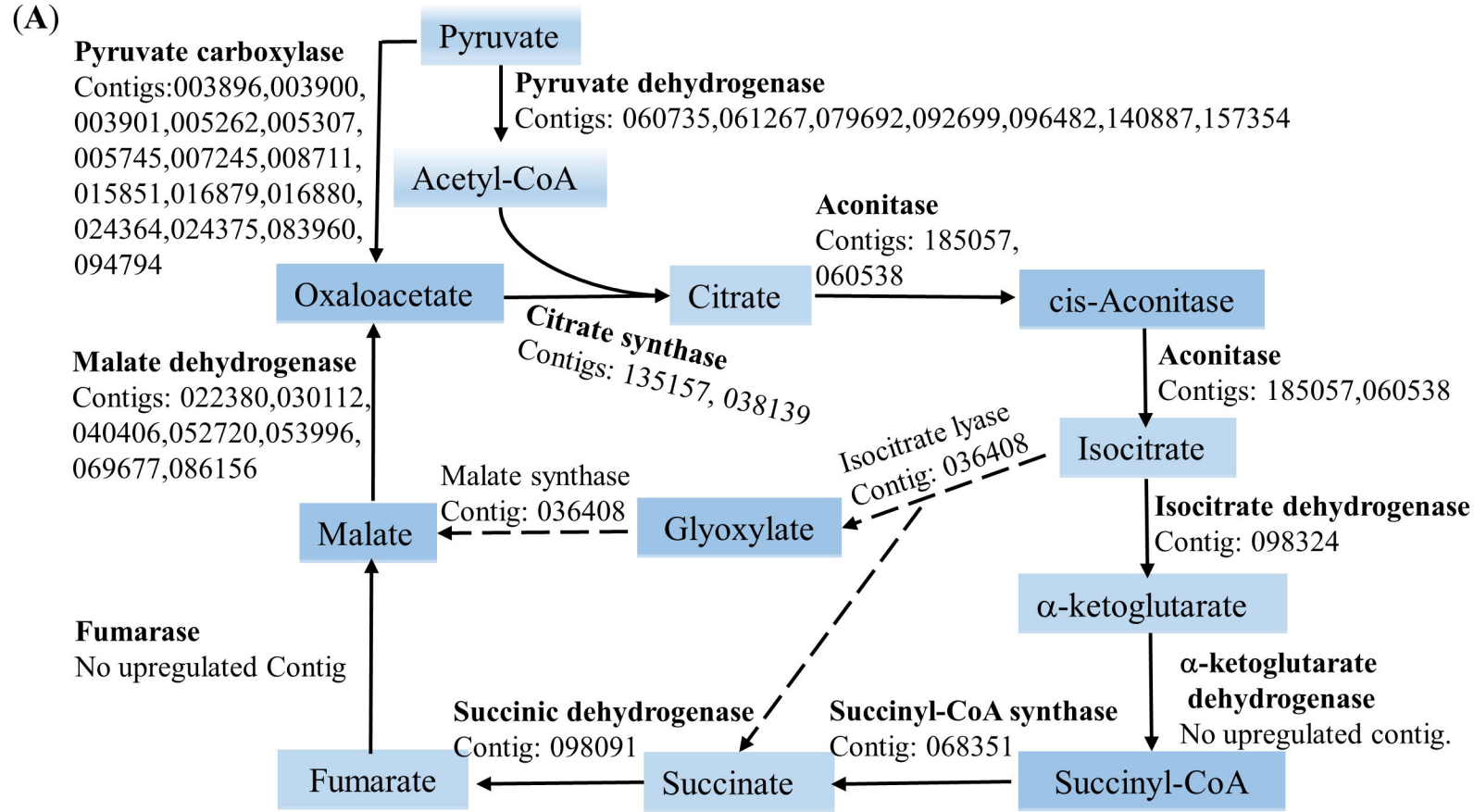

Wang *et al.*, Fig. 5A

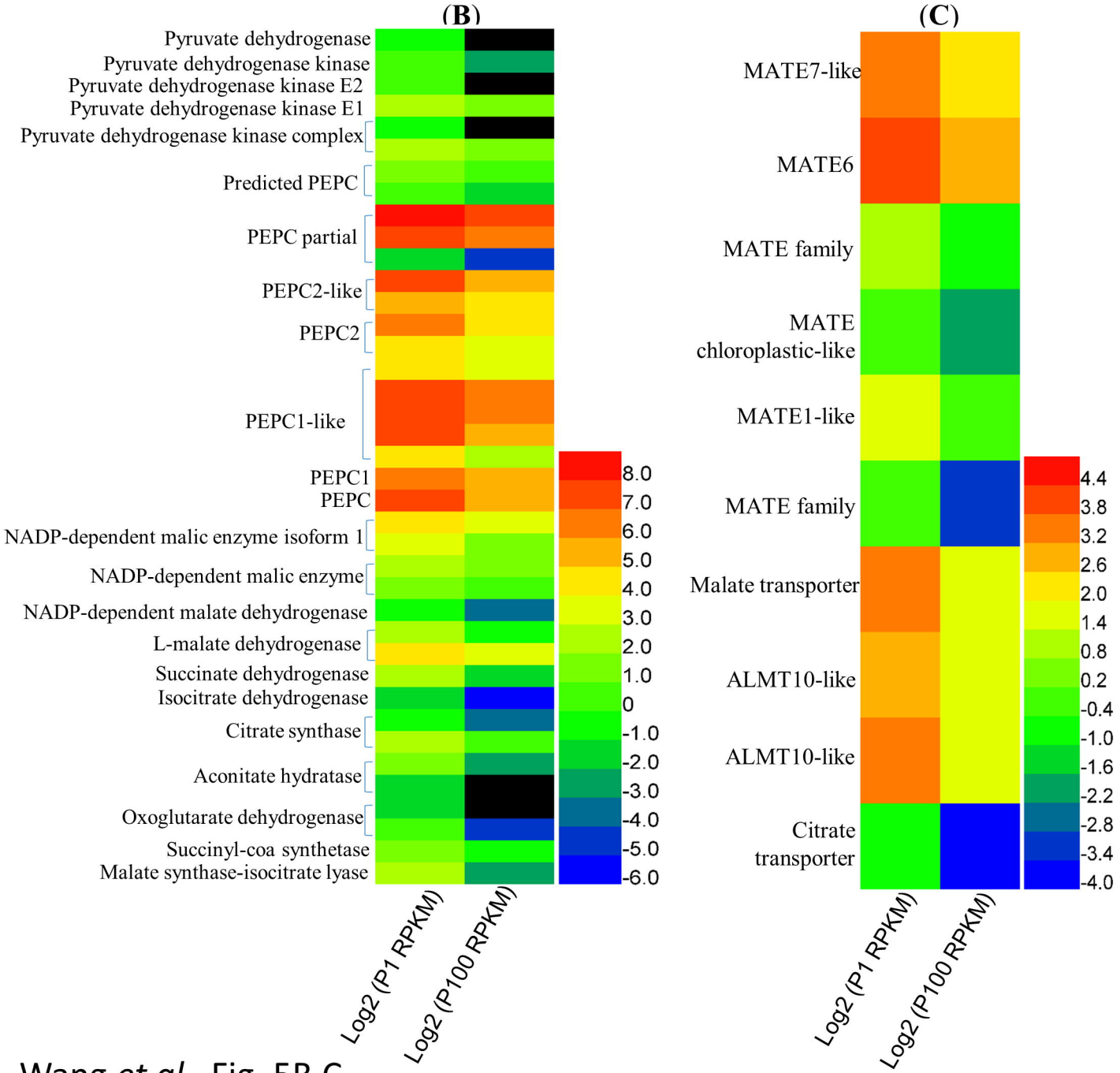

Wang *et al.*, Fig. 5B,C

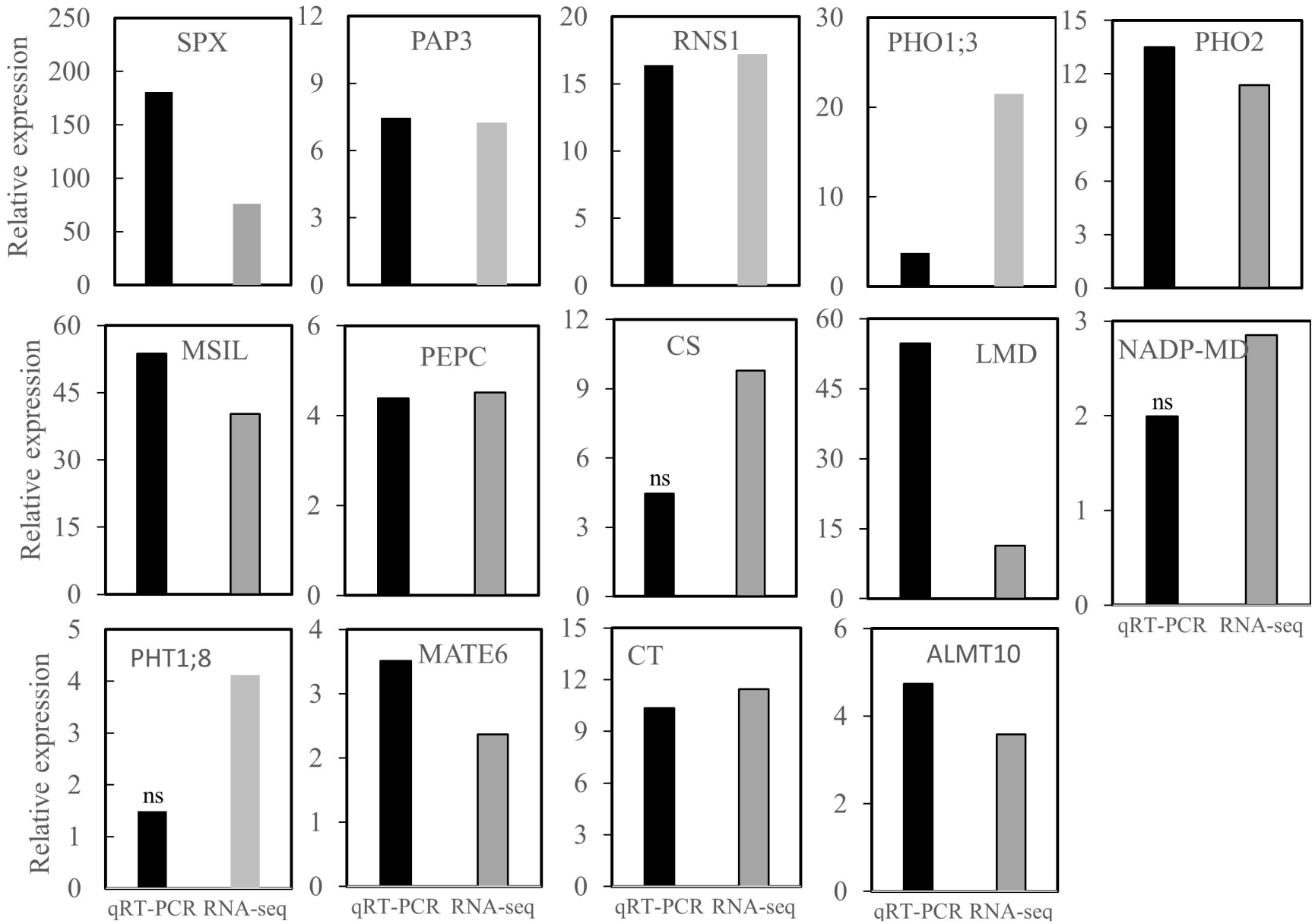

Wang *et al.*, Fig.6

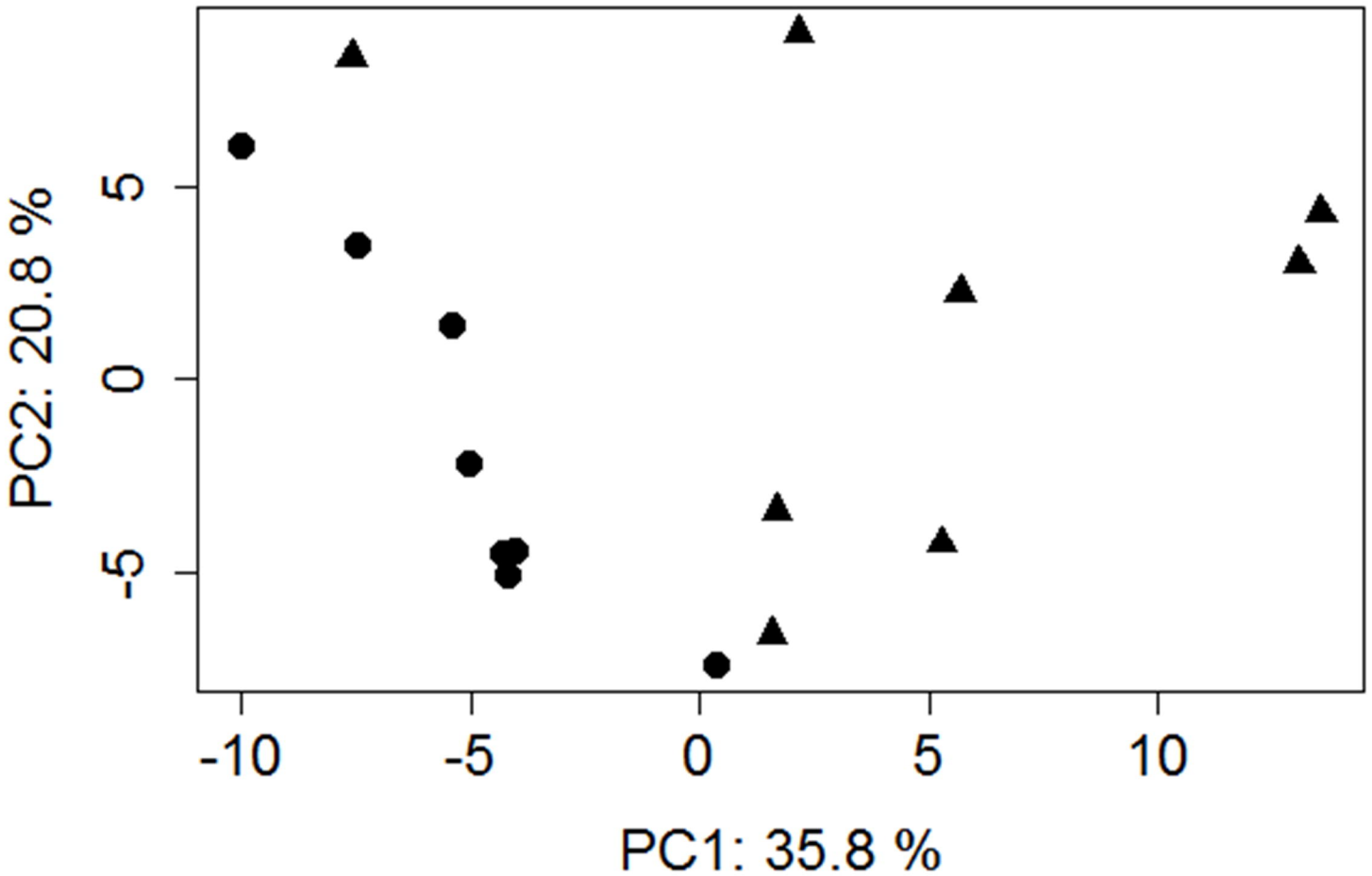

Wang *et al*., Fig.7